ELSEVIER

Journal of Fluorine Chemistry 113 (2002) 37–45

JOURNAL OF FLUORINE CHEMISTRY

www.elsevier.com/locate/jfluchem

The nature of anionic clusters in anion excess fluorite-type oxidefluoride solid solutions in MF–BiF_3–BiOF systems (M = Na, K)

M. El Omari[a], J.M. Réau[b], J. Sénégas[b,*], T.V. Serov[c], E.I. Ardashnikova[c], V.A. Dolgikh[c]

[a]*Department of Chemistry, Faculty of Science, Moulay Ismaïl University, Meknes, Morocco*
[b]*Institut de Chimie de la Matière Condensée de Bordeaux (ICMCB), 87 Avenue Dr. A. Schweitzer, 33608 Pessac Cedex, France*
[c]*Chemistry Faculty, Lomonosov Moscow State University, Vorobjovy Gory, Moscow 119899, Russia*

Received 29 May 2001; accepted 21 June 2001

Abstract

Various compositions of the range of fluorite-type oxidefluoride solid solution in the NaF–BiF_3–BiOF system are investigated by ^{19}F NMR spectroscopy. Using the following formulation, $Na_{0.5(1-z-h)}Bi_{0.5(1+z+h)}F_{2+z-h}O_h$, this study is undertaken as a function of the anion excess (z) and the oxygen content (h). It results in the existence of two fluoride sublattices in the solid solution range. An approach to the nature of the fluorine–oxygen order is proposed when the compositions become richer and richer in BiOF. The clustering model is then extended to the homologous potassium oxidefluoride solid solutions. © 2002 Elsevier Science B.V. All rights reserved.

Keywords: Oxidefluorides; F^- ion conductors; ^{19}F NMR spectroscopy; Clustering

1. Introduction

A wide range of anion excess fluorite-type oxidefluoride solid solution has been shown in the NaF–BiF_3–BiOF system; it extends from the entirely fluoride $Na_{0.5(1-z)}Bi_{0.5(1+z)}F_{2+z}$ solid solution along the (NaF–BiF_3) line towards BiOF [1]. The various range compositions can be formulated $Na_{0.5(1-z-h)}Bi_{0.5(1+z+h)}F_{2+z-h}O_h$ in the system of oblique axes (Oz, Oh), where $NaBiF_4$ is the origin, O and the ($NaBiF_4$–BiOF) and ($NaBiF_4$–BiF_3) lines, are respectively the Oh and Oz axes (Fig. 1): the variables z and h represent, respectively the anion excess and the oxygen content. Composition dependence of electrical properties has been studied in preliminary work along two particular lines characterised, the one (δ_2), by a fixed value of z ($z = 0.26$), the other (δ_4), by the ($z + h = 0.60$) relation, i.e. the value 0.25 of the Na/Bi ratio. Considering the modes of formal substitution along the (δ_2) and (δ_4) lines:

$$(\delta_2)\ \text{line}: \quad Na^+ + 2F^- \rightarrow Bi^{3+} + 2O_2{}^- \quad (\text{as } h \text{ increases}),$$

$$(\delta_4)\ \text{line}: \quad 2F^- \rightarrow O_2{}^- \quad (\text{as } h \text{ increases}),$$

the conductivity is more influenced by cationic substitution than the anionic and a decrease of transport properties is observed when the bismuth content increases [1]. On the other hand, an ^{19}F NMR investigation of some compositions along the (δ_2) line has proved the existence at low temperatures of two fluoride sublattices (F_n) and (F_i), in these sodium oxidefluoride materials and suggested the presence of cubo-octahedral $(F_i)_{12}$ clusters analogous with those shown in $K_{0.5(1-z)}Bi_{0.5(1+z)}F_{2+z}$ [1,2].

The conductivity drops observed along each axis when the variables h or z increase are associated with an increase with z of $n(F_i)$, the number of interstitial fluoride ions and, on the contrary, to a decrease with h of $n(F_i)$: consequently, they are not caused by the same effect. The decrease of $n(F_i)$ with increasing h along (δ_2) parallel to Oh should involve a lowering of the number of cubo-octahedral entities which is in favour of a higher conductivity; the conductivity decrease observed could then be due to the progressive setting up of an order of unlike nature, a fluorine–oxygen order for instance.

This paper deals with a more complete study of F^- ion diffusion properties in the sodium oxidefluoride solid solution in order to confirm the preliminary results obtained; the elongated shape of the oxidefluoride range has incited us to select the particular lines (δ_5) and (δ_6), joining entirely fluoride compositions to BiOF (Fig. 1). An approach to the nature of the fluorine–oxygen order is then proposed and such an approach is extended to the homologous potassium solid solution shown in the KF–BiF_3–BiOF system [3].

* Corresponding author. Tel.: +33-556-846-260; fax: +33-556-842-761.
E-mail address: senegas@icmcb.u-bordeaux.fr (J. Sénégas).

0022-1139/02/$ – see front matter
PII: S0022-1139(01)00467-5

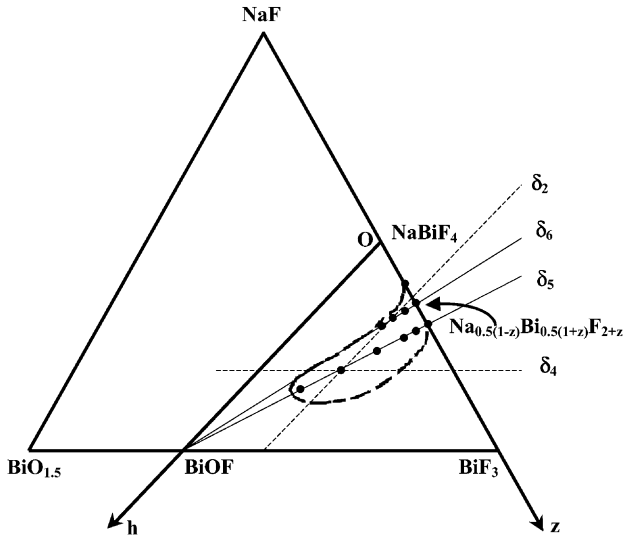

Fig. 1. Range of oxyfluoride solid solution with fluorite-type structure in the $NaF–BiF_3–Bi_2O_3$ system.

2. Experimental

The starting materials were high-purity (>99.9%) sodium and bismuth fluorides and bismuth oxide. NaF was dried at 423 K for 2 h and kept in a dessicator over P_2O_5. BiF_3 was prepared from Bi_2O_3 by reaction with aqueous HF (40%) and the precipitate obtained was heated at 673 K for 3 h under a flow of anhydrous HF [4,5]. The mixed powders of NaF, Bi_2O_3 and BiF_3, taken in appropriate ratios, were ground in the dry box and introduced into metal tubes. Copper, gold or platinum were used as tube materials, as use of these metals had given reproducible results during the former experiments [1]. After degassing in a dynamic vacuum for 2 h and filling with dry argon, the tubes were sealed, heated at 723 ± 10 K for 12 h and finally quenched in ice water. X-ray powder diffraction analysis was performed with a Guinier camera FR-552 (Cu $K\alpha_1$ radiation) using germanium as internal standard.

Ionic conductivity measurements were carried out on powder samples pressed to form pellets sintered under the same operating conditions as for synthesis. The samples are of cylindrical form (diameter: ≈8 mm; and thickness: $1\text{ mm} < t < 2\text{ mm}$). Gold or copper were used as electrode materials on both sides of the pellets. The electrical properties were determined using a Solartron 1250 frequency response analyser associated with a Solartron 1286 electrochemical interface. The frequency range was 10^0 to 10^6 Hz and measurements were carried out under dry argon over the thermal interval (293–573 K) in several temperature cycles. Complex impedance diagrams obtained for each temperature were treated by the equivalent circuit method using non-linear least-squares fitting.

^{19}F NMR experiments were performed on a Bruker MSL-200 spectrometer ($B_0 = 4.7$ T) equipped with a standard variable temperature unit in the temperature range (175–400 K).

Table 1
Experimental conditions of the ^{19}F NMR investigation of the studied materials

Spectrometer frequency (MHz)	188.283
Pulse width (μs)	0.7
Dead time delay (μs)	6
Recycle delay time (s)	10
Spectral width (MHz)	1
Filter width (MHz)	1

For each temperature of measurement, the powder samples are kept for 1 h at that temperature, in order to attain a good thermal stability. Storage over 1 h of a large number of acquisitions allowed high resolution signals to be registered. The ''ONEPULSE'' acquisition program [6] was used in the operating conditions listed in Table 1. This program was selected because it delivers a spectral irradiation large enough to cover the different spectral widths of each type of F^- ions. In fact, different diffusion coefficients characterise the F^- ions in the materials used. Signals obtained were processed by Fourier transformation, using the ''WINNMR 1D'' program [7].

Simulations of the ^{19}F NMR lines were performed using the ''WINFIT'' program [8]. This program allows the adjustment of the peak position, peak height and line width ratio of Gaussian and Lorentzian functions and the relative percentage of their areas. When a single Gaussian does not fit exactly with the registered spectrum, an appropriate mixing of Gaussian and Lorentzian functions is used for the simulation. It was particularly, the case for the spectra corresponding to the motional narrowing temperature range.

3. Results

3.1. Electrical properties

The selected (δ_5) and (δ_6) lines, are respectively the ($Na_{0.30}Bi_{0.70}F_{2.40}$–BiOF) and ($Na_{0.35}Bi_{0.65}F_{2.30}$–BiOF) lines (Fig. 1). Along these lines, the z and h variables comprise the following relations:

$$(\delta_5): \quad 17z + 7h = 6.80; \qquad (\delta_6): \quad 3z + h = 0.90$$

The various compositions located on these particular lines can be written as a function of h only:

$$(\delta_5): \quad Na_{0.5(0.60-10h/17)}Bi_{0.5(1.40+10h/17)}F_{2.40-24h/17}O_h \quad (0 < h < 0.50)$$

$$(\delta_6): \quad Na_{0.5(0.70-2h/3)}Bi_{0.5(1.30+2h/3)}F_{2.30-4h/3}O_h \quad (0 < h < 0.44)$$

In the temperature range studied (293–573 K), the conductivity data for each sample offer an Arrhenius-type behaviour; a linear fit to $\sigma T = \sigma_0 \exp(-\Delta E_\sigma / kT)$ is shown with a correlation coefficient equal to 0.98. Variation of $\log \sigma_{373\text{ K}}$

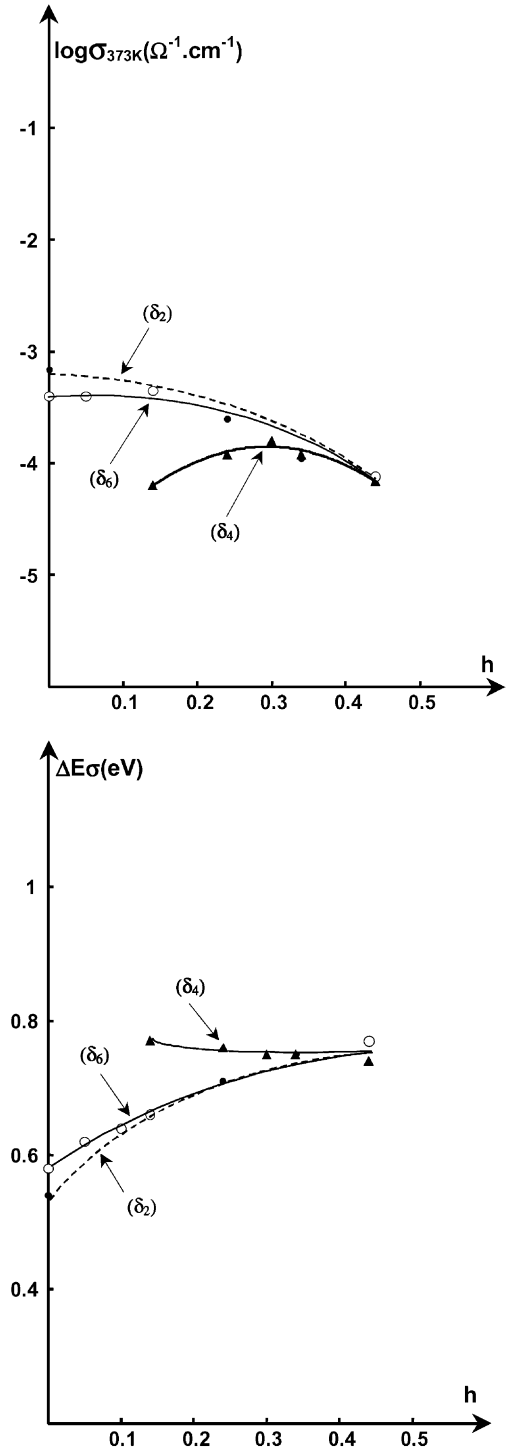

Fig. 2. Variation of $\log \sigma_{373\ \mathrm{K}}$ and ΔE_σ as a function of h for various compositions located along the (δ_2), (δ_4) and (δ_6) lines.

and ΔE_σ as a function of h is given in Fig. 2 for some compositions on the (δ_6) line: a decrease of conductivity associated with an increase of ΔE_σ is clearly shown when h increases along that line. The results previously obtained for the compositions located on the (δ_2) and (δ_4) lines [1] are also reported for comparison in Fig. 2: whatever the line selected, the electrical properties seem to tend towards a same value for the high values of h.

3.2. ^{19}F NMR investigation

The ^{19}F NMR spectra at various temperatures between 175 and 400 K are given, as examples, in Fig. 3a, for three particular compositions located on the (δ_5) line and corresponding to $h = 0.10$, 0.34 and 0.50.

At very low temperatures, two peaks, labelled p_1 and p_2, are detected at frequencies of approximately +5 and −30 kHz, respectively. The origin of the frequency scale corresponds to the nominal irradiation frequency (188.28 MHz). The whole spectrum relative to a fixed temperature can be simulated with the help of two Gaussian functions (Fig. 3b), which means that all F^- ions are fixed over the NMR time scale in this temperature range and belong to two separate fluoride sublattices. The p_1 and p_2 peaks have been attributed, whatever the h value, to fluoride ions localised, respectively in the (F_n) normal and (F_i) interstitial sites of the fluorite-type lattice. Above $T \approx 200$ K, a new peak, p_m, located between p_1 and p_2, can be seen, where it is growing with increasing temperature at the expense of both others. Simulated by a Lorentzian function, p_m represents the mobile fluoride ions. At $T \approx 400$ K, only a p_m peak is observed, the F^- ions are consequently, all mobile over the NMR time scale above that temperature.

The variation of the ^{19}F NMR spectral width at half-height ($\Delta v^{1/2}$) over the same thermal range is given in Fig. 4. The plateau at low temperatures corresponds to the linewidth of the rigid lattice (Δv_R). Above $T \approx 200$ K, $\Delta v^{1/2}$ decreases progressively when temperature increases. The narrowed linewidth is due to mobile F^- ion motions that average out the F–F dipolar interactions. Above $T \approx 380$ K, $\Delta v^{1/2}$ reaches the limit (Δv_r) determined by experimental magnetic-field inhomogeneities.

The experimental points for each sample are located on a curve which can be simulated by the Boltzman function:

$$\Delta v^{1/2}(T) = \Delta v_r + \frac{\Delta v_R - \Delta v_r}{1 + \exp|(T - T_0)/\Delta T|}$$

where Δv_R and Δv_r are defined above, T_0 is the centre of the Boltzman function, and $\Delta T = \sum(T_i - T_j)/n$ is the average temperature difference between two successive temperatures T_i and T_j, with $(n + 1)$ the number of measurement temperatures. The values of various calculated parameters for the three samples are given in Table 2.

The activation energy of mobile F^- ion relaxation was calculated for each sample from the thermal variation of the jump frequency, v_s. Line narrowing occurs when the v_s frequency is of the same order as the rigid lattice linewidth. The thermal variation of v_s may be deduced from that of $\Delta v^{1/2}$ from the expression [9]

$$v_s = \frac{\alpha|\Delta v^{1/2} - \Delta v_r|}{\tan|\pi/2[(\Delta v^{1/2} - \Delta v_r)/(\Delta v_R - \Delta v_r)]^2|}$$

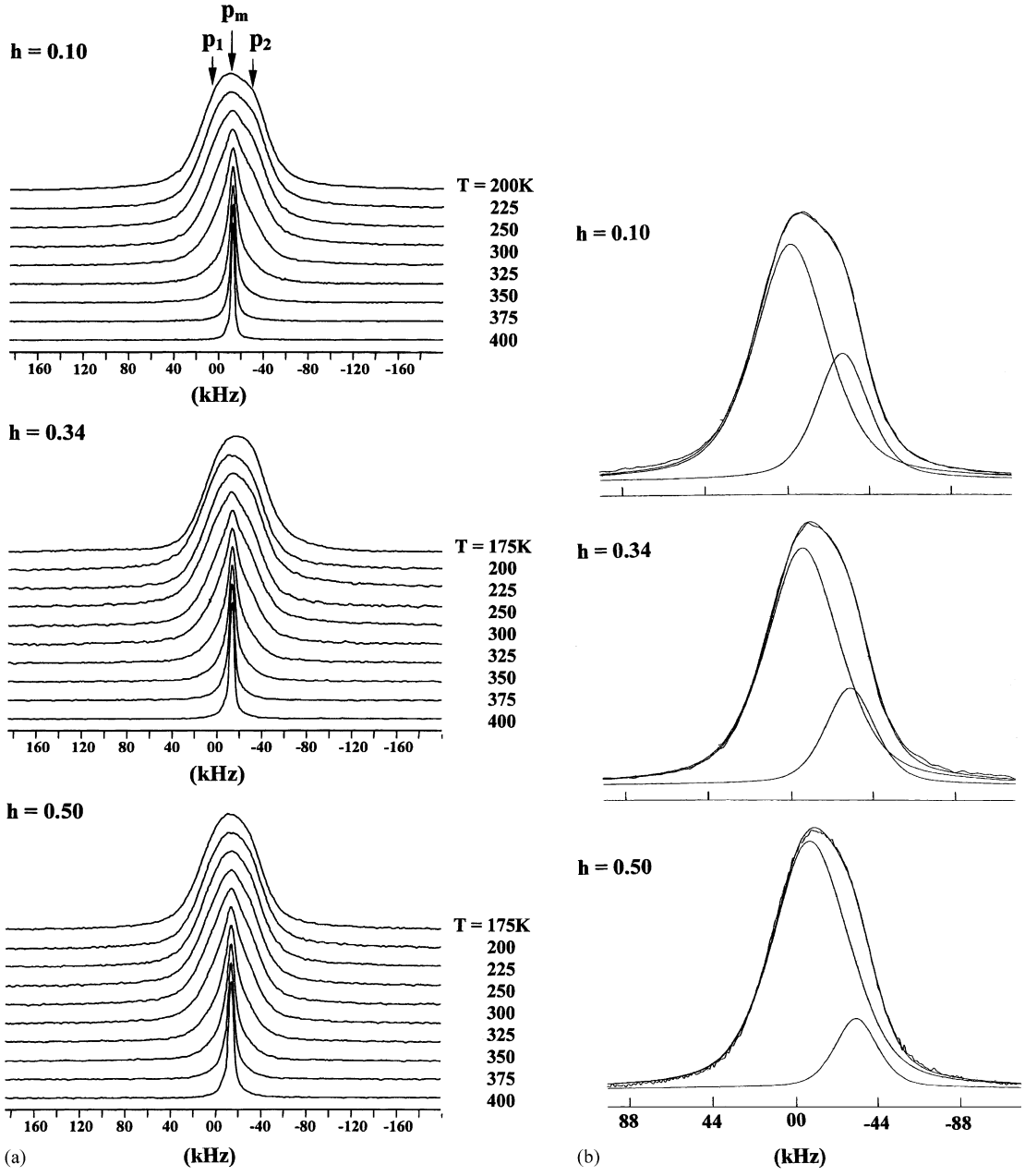

Fig. 3. (a) Thermal variation of the ^{19}F NMR spectrum for the compositions $Na_{0.5(0.60-10h/17)}Bi_{0.5(1.40+10h/17)}F_{2.40-24h/17}O_h$ corresponding to $h = 0.10$, 0.34 and 0.50; (b) deconvolution of the ^{19}F NMR spectra at low temperatures for the compositions $Na_{0.5(0.60-10h/17)}Bi_{0.5(1.40+10h/17)}F_{2.40-24h/17}O_h$ corresponding to $h = 0.10$, 0.34 and 0.50.

where $\Delta v^{1/2}$ is the halfwidth measured at temperature T, Δv_R and Δv_r have been defined above, and α is a constant function of line shape. The Gaussian line shape at low temperature led to a choice of $\alpha = 1$. Temperature dependence of v_s over the range $200\,K \leq T \leq 375\,K$ is given for the three samples in Fig. 5: v_s follows an Arrhenius-type relation with $v_s = v_0 \exp(-\Delta E_{NMR}/kT)$ on either side of the transition temperature, T_r. The energies in the $T < T_r$ and $T > T_r$ temperature ranges, as well as the T_r temperatures are reported in Table 2 for the three samples studied.

The results obtained from the ^{19}F NMR investigation of some compositions located along the (δ_5) line confirm the results obtained in a preliminary work with compositions located along the (δ_2) line [1]. Analogous results have also been obtained with compositions located on the (δ_6) line. The various diffusion and simulation parameters deduced from the ^{19}F NMR investigation of samples located on the (δ_5) and (δ_6) lines are reported in Table 2.

3.3. Discussion

The ^{19}F NMR investigation of compositions located inside the range of oxidefluoride solid solution in the $NaF–BiF_3–Bi_2O_3$ system proves the presence of two fluoride

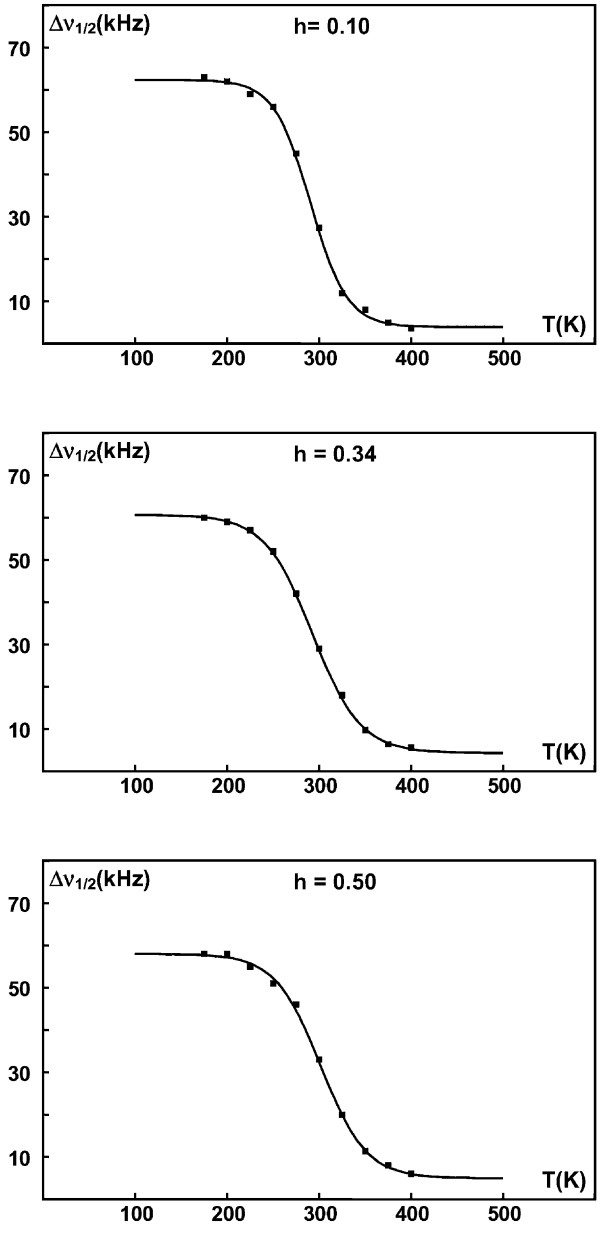

Fig. 4. Temperature dependence of the $\Delta\nu^{1/2}$ (kHz) linewidth for the compositions $Na_{0.5(0.60-10h/17)}Bi_{0.5(1.40+10h/17)}F_{2.40-24h/17}O_h$ corresponding to $h = 0.10$, 0.34 and 0.50.

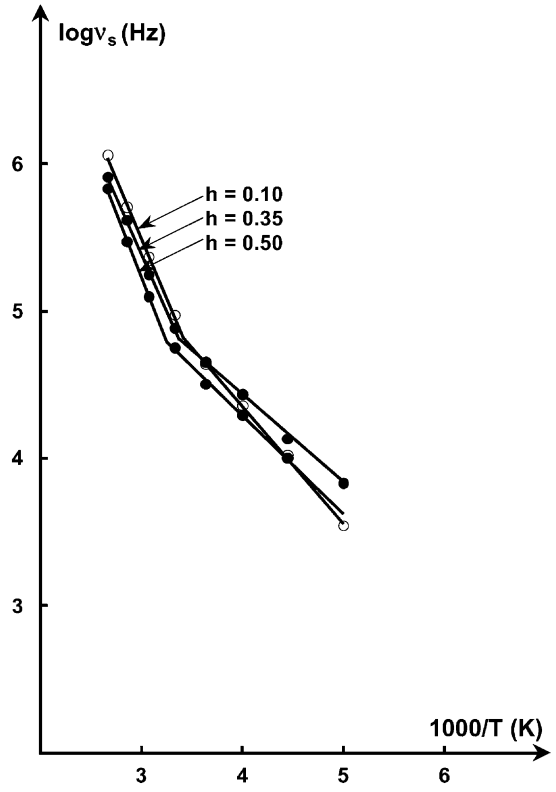

Fig. 5. Inverse temperature dependence of log v_s for the compositions $Na_{0.5(0.60-10h/17)}Bi_{0.5(1.40+10h/17)}F_{2.40-24h/17}O_h$ corresponding to $h = 0.10$, 0.34 and 0.50.

sublattices, whatever the h value. On the other hand, the values of $n(F_n)$ and $n(F_i)$ for the entirely fluoride compositions ($h = 0$) located on the (δ_2), (δ_5) and (δ_6) lines, are respectively close to the numbers of fluoride ions located in the normal positions and the interstitial sites of F′ type determined by neutron diffraction for the potassium fluoride composition $K_{0.40}Bi_{0.60}F_{2.20}$: $n(F_n) = 1.36$, $n(F') = 0.84$ [2]. This result suggests that the (F_i) interstitial fluoride ions in $Na_{0.5(1-z)}Bi_{0.5(1+z)}F_{2+z}$ could also be of F′ type. It is then possible to consider in $Na_{0.5(1-z)}Bi_{0.5(1+z)}F_{2+z}$, as in $K_{0.5(1-z)}Bi_{0.5(1+z)}F_{2+z}$, the existence of cubic $(F_n)_8$ and cubo-octahedral $(F')_{12}$ entities and to explain the composition dependence of electrical properties: inside the sodium fluoride solid solution, the decrease in electrical performance is due, as in the potassium fluoride solid solution, to the setting up of an more and more extended order between both entities when z increases.

The values of ΔE_{NMR} calculated on both sides of T_r ($\approx$0.14 eV in the $T < T_r$ range and $\approx$0.29 eV in the $T > T_r$ range) for compositions located along the (δ_5) and (δ_6) lines are very close to those obtained for compositions located on the (δ_2) line [1] and do not vary much when h increases. Whatever the studied line, the ΔE_{NMR} values are clearly lower than those of ΔE_σ. Consequently, the F^- ion motions over the NMR time scale are short range. In the $T < T_r$ temperature range, the very small value of ΔE_{NMR} could possibly be attributed to local F^- ion motions inside the cubo-octahedral entities, for instance. In the $T > T_r$ temperature range, the higher value of ΔE_{NMR} could then correspond to exchange motions between cubic entities and cubo-octahedral clusters.

3.4. What local order inside the oxyfluoride solid solution range?

In preliminary work [1], we have shown that the conductivity decrease observed along the Oz axis and the (δ_2) line parallel to the Oh axis cannot have the same origin as they are associated with an increase with z of $n(F_i)$ and, on the contrary, to a decrease with h of $n(F_i)$. The increase of

Table 2
Diffusion and simulation parameters deduced from the ^{19}F NMR investigation of various compositions located on the (δ_5) and (δ_6) lines.

h	$\%p_1$ (175 K) (±3)	$\%p_2$ (175 K) (±3)	$n(F_n)$ (±0.03)	$n(F_i)$ (±0.03)	$n(F+O)_n$ (±0.03)	$\Delta\nu_R$ (kHz)	$\Delta\nu_r$ (kHz)	T_0 (K)	ΔT (K)	ΔE_{NMR} (eV) ($T < T_r$) (±0.02)	ΔE_{NMR} (eV) ($T > T_r$) (±0.02)	T_r (K) (±2)
$Na_{0.5(0.60-10h/17)}Bi_{0.5(1.40+10h/17)}F_{2.40-24h/17}O_h$ compositions—(δ_5) line												
0	62	38	1.49	0.91	1.49	64.49	2.85	287	24.90	0.13	0.26	271
0.05	68	32	1.59	0.74	1.64	62.40	4.45	287	20.13	0.15	0.29	272
0.10	72	28	1.63	0.63	1.73	62.33	3.91	291	19.88	0.15	0.30	275
0.20	74	26	1.58	0.54	1.78	60.63	4.33	290	21.55	0.16	0.32	292
0.34	78	22	1.51	0.41	1.85	60.62	4.31	293	26.10	0.12	0.31	294
0.50	87	13	1.48	0.22	1.98	57.96	4.94	302	24.73	0.13	0.35	308
$Na_{0.5(0.70-2h/3)}Bi_{0.5(1.30+2h/3)}F_{2.30-4h/3}O_h$—($\delta_6$) line												
0	61	39	1.41	0.89	1.41	61.52	4.89	264	19.58	0.13	0.28	264
0.05	68	32	1.52	0.71	1.57	62.21	4.75	267	19.89	0.14	0.30	268
0.10	68	32	1.49	0.68	1.59	61.70	4.37	269	21.56	0.14	0.26	269
0.14	69	31	1.47	0.65	1.61	59.92	4.92	275	19.57	0.14	0.30	269

$n(F_i)$ with z is associated with the increase of cubo-octahedral entities which trap the charge carriers and are favourable to the establishment of a more and more developed order between the cubic and cubo-octahedral entities. On the contrary, the decrease of $n(F_i)$ with increasing h along (δ_2) should involve a reduction of the number of cubo-octahedral entities which is in favour of a higher conductivity. In order to elucidate the conductivity decrease observed, one could consider the progressive setting-up of an order of unlike nature, a fluorine–oxygen order for instance, inside the oxidefluoride solid solution [1].

The investigation of electrical and diffusion properties by impedance and ^{19}F NMR spectroscopies along the (δ_5) and (δ_6) lines has shown the following results:

- the F^- ion conductivity decreases with increasing h and seems to tend towards a limit in the BiOF direction, for high values of h (Fig. 2);
- the number of $n(F_i)$ decreases regularly with increasing h and involves a progressive decrease of cubo-octahedral entities (Table 2);
- the number of anions $(F + O)_n$ in the normal positions of the fluorite also increases regularly, involving a progressive increase of the number of cubic entities (Table 2).

Consider the compositions located along the (δ_5) line, the range of which is characterised by the widest variation of h parameter ($0 < h < 0.50$) and assume, whatever h, the coexistence of entirely fluoride cubo-octahedral and ''all mixed'' cubic entities containing fluoride and oxygen anions. The percentage of oxygen in these ''all mixed'' entities can be calculated for each h value:

$$\text{oxygen}\,(\%) = \frac{100h}{[n(F_n) + h]}$$

The variation of the oxygen percentage in ''all mixed'' cubic entities as a function of h is given in Fig. 6. This percentage increases regularly when h increases. Its value is close to 25% for $h = 0.50$. The corresponding cubic entity consists of two O and six F atoms located at the apexes of a cube, with the oxygen atoms in diametrically opposite positions along $\langle 1\,1\,0\rangle$ or $\langle 1\,1\,1\rangle$ directions; such a configuration is in good agreement with the existence of an oxygen–fluorine order. That oxidefluoride composition ($h = 0.50$) is located close to the boundary of the range of solid solution, it consists mainly of mixed cubic entities $|[n(F_n) + h)]/8 \approx 0.25|$ with only few cubo-octahedral entities $|n(F_i)/12 \approx 0.02|$. Starting from the entirely fluoride composition ($h = 0$), it appears reasonable to propose the progressive formation with increasing h of mixed cubic entities with the ($O/F = 0.25$) ratio at the detriment at the same time of cubo-octahedral clusters and of entirely fluoride cubic entities. For the h values such as ($0 < h < 0.50$), there would consequently be coexistence of fluoride cubo-octahedrons, entirely fluoride cubic entities and mixed cubic entities with an ($O/F = 0.25$) ratio. The percentages of three types of clusters proposed have been calculated for the various h values and are collected in Table 3. The percentage of the mixed cubic entities increases regularly with increasing h (Fig. 7); this is in agreement with the [$\%p \approx 100(2h)$] relation for the low h values, then, beyond $h \approx 0.10$, it increases less quickly and a more and more important deviation can be observed at the boundary of oxidefluoride solid solution range (Fig. 7).

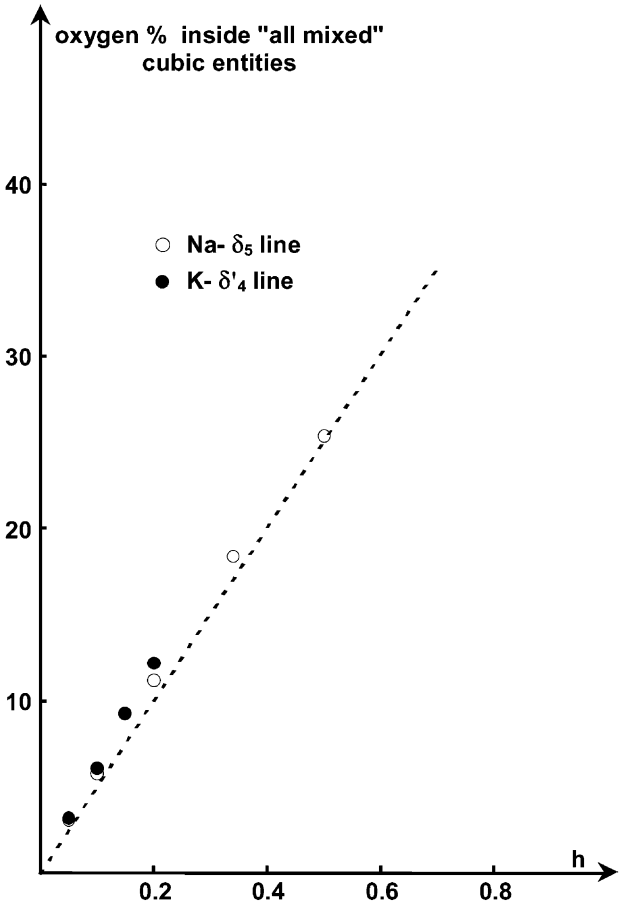

Fig. 6. Variation of oxygen percentage inside ''all mixed'' cubic entities as a function of h, for the $Na_{0.5(0.60-10h/17)}Bi_{0.5(1.40+10h/17)}F_{2.40-24h/17}O_h$ and $K_{0.5(0.64)}Bi_{0.5(1..36)}F_{2.36-2h}O_h$ compositions.

Consider now the results obtained by neutron diffraction investigation for the $K_{0.5(0.64)}Bi_{0.5(1.36)}F_{2.36-2h}O_h$ potassium

Table 3
Percentages of cubo-octahedral, entirely fluoride cubic and mixed cubic entities for various compositions located on the (δ_5) line inside the sodium oxyfluoride solid solution

h	Percentage of cubo-octahedral entities	Percentage of entirely fluoride cubic entities	Percentage of mixed (two O and six F atoms) cubic entities
0	≈29	≈71	≈0
0.05	≈23	≈67	≈10
0.10	≈19	≈62	≈19
0.20	≈17	≈46	≈37
0.34	≈13	≈23	≈64
0.50	≈7	≈0	≈93

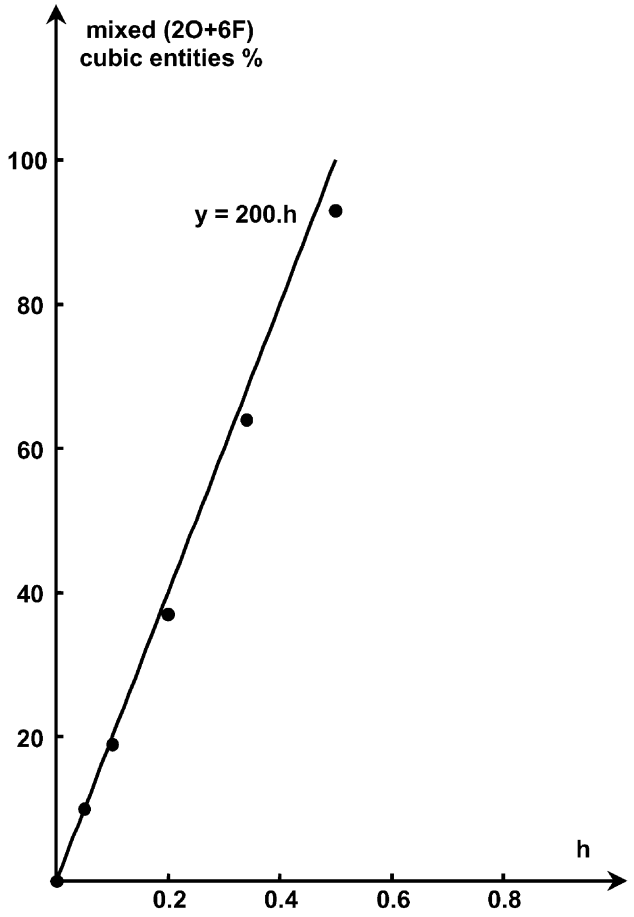

Fig. 7. Variation of the percentage of mixed (two O and six F atoms) cubic entities as a function of h for the $Na_{0.5(0.60-10h/17)}Bi_{0.5(1.40+10h/17)}F_{2.40-24h/17}O_h$ compositions.

compositions located on a (δ'_4) line parallel to the $BiO_{1.5}$–BiF_3 line inside the range of potassium oxidefluoride solid solution of fluorite-type structure. These compositions are characterised by the value $r = 0.47$ of the K/Bi ratio and the $z + h = 0.36$ relation. The formal substitution along the (δ'_4) line is: $2F^- \rightarrow O^{2-}$ when h increases. The potassium oxidefluoride solid solution range is extended, as that of sodium, from the entirely fluoride solid solution $K_{0.5(1-z)}Bi_{0.5(1+z)}F_{2+z}$ towards BiOF (Fig. 8).

Table 4 gives the values of $n(F_n)$ and $n(F')$ determined by neutron diffraction for various $K_{0.5(0.64)}Bi_{0.5(1.36)}F_{2.36-2h}O_h$ compositions. A decrease of $n(F')$ with increasing h is observed in the potassium solid solution range, as in that of sodium, and it results also in a decrease of cubo-octahedral entities in the potassium solid solution. The hypothesis of the establishment of a fluorine–oxygen order when h increases has consequently been investigated inside the potassium solid solution by analogy with that of sodium. The variation of oxygen percentage inside "all mixed" cubic entities as a function of h is given for the $K_{0.5(0.64)}Bi_{0.5(1.36)}F_{2.36-2h}O_h$ compositions in Fig. 6: for a given h

Table 4
Results obtained from neutron diffraction investigation of some $K_{0.5(0.64)}Bi_{0.5(1.36)}F_{2.36-2h}O_h$ compositions [3]

h	$n(F_n)$	$n(F')$
0	1.44	0.92
0.05	1.56	0.70
0.10	1.54	0.62
0.15	1.48	0.57
0.20	1.43	0.53

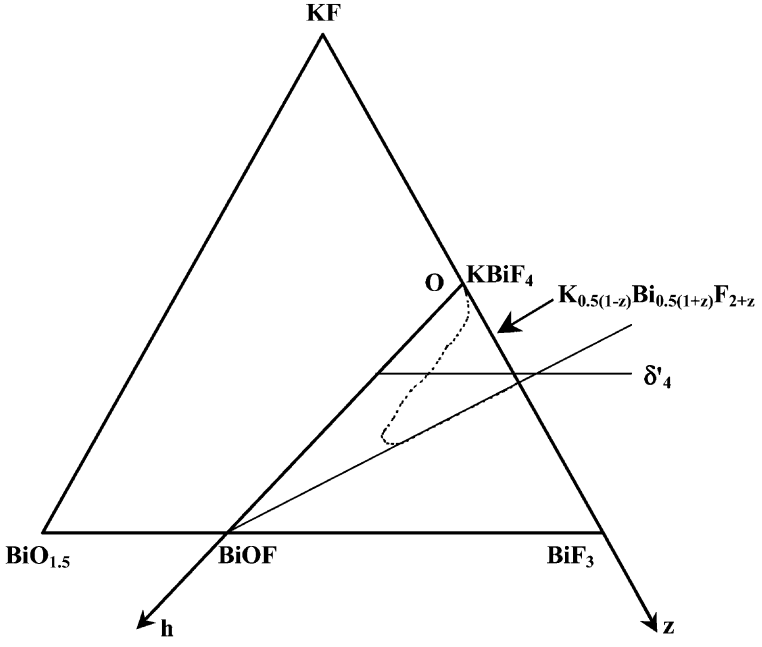

Fig. 8. Range of oxyfluoride solid solution with fluorite-type structure in the KF–BiF_3–Bi_2O_3 system [3].

Table 5
Percentages of cubo-octahedral, entirely fluoride cubic and mixed cubic entities for various compositions located on the (δ'_4) line inside the potassium oxyfluoride solid solution

h	Percentage of cubo-octahedral entities	Percentage of entirely fluoride cubic entities	Percentage of mixed (two O and six F atoms) cubic entities
0	≈30	≈70	≈0
0.05	≈23	≈70	≈7
0.10	≈21	≈64	≈15
0.15	≈20	≈56	≈34
0.20	≈20	≈46	≈34

value, the points representative of potassium solid solution are very close to and slightly higher than those for to the sodium solid solution. It is very probable that the potassium oxidefluoride solid solution offers, as that of sodium, the three types of entities $(F')_{12}$ cubo-octahedral, entirely fluoride cubic entities and mixed cubic entities containing two O and six F atoms. The percentages of the three different entities, calculated for each composition, are reported in Table 5 for the potassium solid solution. For a same h value, the values of percentages obtained for the two solid solutions are very close. Such a result, obtained from a ^{19}F NMR investigation for the sodium solid solution and from a neutron diffraction study for that of potassium, confirms the presence of the same clustering type inside both oxidefluoride solid solutions.

4. Conclusions

^{19}F NMR investigations of various compositions located inside the range of oxidefluoride solid solution in the NaF–BiF_3–BiOF system has proved the presence at low temperatures of two fluoride sublattices. The existence of cubic and cubo-octahedral entities in the sodium oxidefluoride solid solution has been suggested by analogy with the homologous potassium solid solution. The F^- ion motions over the NMR time scale are short range. Two types of F^- ion motions have been revealed at increasing temperature from the temperature dependence of the jump frequency: the first, at low temperatures are weakly activated and could be interpreted as motions inside clusters; the second, at higher temperatures, are characterised by a higher activation energy and could correspond to exchange motions between both sublattices.

The F^- ion conductivity decrease observed with the increasing oxygen content (h) tends towards a limit in the BiOF direction, for the high values of h. That variation of conductivity is associated with a progressive increase in the number of cubic entities to the detriment of cubo-octahedral entities. An oxidefluoride cubic entity with six F and two O atoms located in the apexes of a cube, the oxygen atoms being in diametrically opposite positions, has been proposed for the limiting composition. It results in the coexistence of fluoride cubo-octahedrons, entirely fluoride cubic entities and mixed cubic entities with the (O/F = 0.25 ratio), inside the whole of the solid solution range. That model, extended to the homologous potassium solid solution range inside the KF–BiF_3–BiOF system, results in the probable presence of the same clustering type as in the sodium oxidefluoride solid solution. It is interesting to note the very large agreement in coherence of results obtained from an ^{19}F NMR investigation in the case of the sodium solid solution and from a neutron diffraction study in the case of the potassium solid solution.

References

[1] T.V. Serov, R.Ya. Zakirov, E.I. Ardashnikova, V.A. Dolgikh, M. El Omari, J. Sénégas, J.M. Réau, Solid State Ionics 138 (2001) 233.
[2] J.L. Soubeyroux, J.M. Réau, S. Matar, G. Villeneuve, P. Hagenmuller, Solid State Ionics 6 (1982) 103.
[3] J.L. Soubeyroux, P. Laborde, J.M. Réau, P. Hagenmuller, J. Solid State Chem. 73 (1988) 217.
[4] C. Lucat, Ph. Sorbe, J. Portier, J.M. Réau, P. Hagenmuller, J. Grannec, Mater. Res. Bull. 12 (1977) 145.
[5] E.I. Ardashnikova, M.P. Borzenkova, F.V. Kalichenko, A.V. Novoselova, Russ. J. Inorg. Chem. 26 (1981) 1727.
[6] ONEPULSE program, Products for spectrometer Type MSL-200, Bruker Spectrospin S.A., Wissembourg, France.
[7] WINNMR 1D program, 1D NMR data processing, version 950901.1, no. SPP-501, Bruker Spectrospin S.A., Wissembourg, France.
[8] WINFIT program, Line shape fitting, version 9504 25, no. SPP-505, Bruker Spectrospin S.A., Wissembourg, France.
[9] N. Bloembergen, E.M. Purcell, R.V. Pound, Phys. Rev. 73 (1948) 679.